Bayasgalan et al, 2021. Mongolian Geoscientist 26 (53) 18-36
DOI: https://doi.org/10.5564/mgs.v26i53.1788

Mongolian Geoscientist

Original Article

Geochemistry and geochronology of granitoid rocks of the Taatsiin Gol pluton of the Khangai Complex, Central Mongolia

Tsogoo Bayasgalan[1]*, Baatar Munkhtsengel[2], Sodnom Khishigsuren[2], Battur Khurelbaatar[1]

[1]* *Gurvan Undes LLC,14200, Ulaanbaatar, Mongolia*
[2] *Department of Geology and Hydrogeology, School of Geology and Mining Engineering, Mongolian University of Science and Technology, Ulaanbaatar 14191, Mongolia*

**Corresponding author: ts.baysgalan0206@gmail.com, ORCID: 0000-0003-4782-4931*

ARTICLE INFO

***Article history*:**
Received 1 October, 2021
Accepted 25 December, 2021

ABSTRACT

The Taatsiin Gol pluton is one of the major constitute the intrusive body of the Khangai Complex, and is composed the first phase of diorite, the second phase of porphyritic granite, biotite-hornblende granite, and granodiorite, and the third phase of biotite granite and alkali granite. This paper presents new geochemical and U-Pb zircon age data from intrusive rocks of the Taatsiin Gol pluton. Geochemical analyses show that the granitoid rocks of the pluton are high-K calc-alkaline, and metaluminous to weakly peraluminous I-type granites, depleted in HFSE such as Nb, Ta, Ti and Y and enriched in LILE such as Rb, Cs, Th, K and LREE, where some variations from early to later phases rock. Zircon U-Pb dating on the biotite granite of the third phase yielded weighted mean ages of 241.4±1.2 Ma and 236.7±1.4 Ma. Based on the new and previous researchers' age results, the age of the Taatsiin Gol pluton of the Khangai Complex is 256-230 Ma consistent with the late Permian to mid-Triassic time. Although showing variated geochemical features, the rocks of the three phases are all suggested to form at an active continental margin setting, probably related to the southwestward subduction of the Mongol-Okhotsk Ocean plate during the late Permian to mid-Triassic period.

Keywords: Mongol-Okhotsk, subduction, active continental margin

INTRODUCTION

Mongolian territory is situated in the central part of the Central Asian Orogenic Belt (CAOB), which is bounded by the Siberian and the East European cratons in the north and the North China and the Tarim cratons in the south (Xiao et al., 2015; Badarch et al., 2002; Windley et al., 2007).

The formation time of the Khangai Complex has long been an issue of debate. In the past, the Khangai Complex was considered to be Paleozoic or older in age for a long time. Taking the Taatsiin Gol pluton, one major constitute the intrusive body of the Khangai Complex, as an example, it was mapped as the Tarvaragtai Complex and was designated a Carboniferous age in the 1:200,000 L-47-72 map Sheet (Tumurchudur et al., 1990), but was regarded as the Proterozoic in the L-48-61 Sheet (Togtokh et al., 1984), as the granitic rock of the Khangai Complex in the L-47-84 Sheet (Zabotkin et al., 1988), neighboring map sheets. Recently, accompanying accumulation of dating data, the Khangai Complex has been considered to be

mainly formed during the late Permian to Triassic period (Fig. 1; Yarmolyuk and Kozlovskiy, 2013, Yarmolyuk et al., 2008; Orolmaa et al, 2008, Orolmaa and Dolzodmaa, 2019; Dolzodmaa et al., 2020).

The tectonic setting of the Khangai Complex is another major topic for discussion. At present, three main points of view in this regard have been invoked, including mantle plume (Yarmolyuk et al., 2016; Yarmolyuk et al., 2013b; Yarmolyuk and Kovalenko, 2003a, 2003b; Kuzmin et al., 2010), subduction of the Mongol-Okhotsk Ocean plate (e.g., Donskaya et al., 2012; Yarmolyuk et al., 2016; Ganbat et al., 2021), and post-collision (Dolzodmaa et al., 2020).

In order to verify the formation age and determine the tectonic setting of the Khangai Complex, we selected the Taatsiin Gol pluton, which contains rocks of three phases and thus is representative of the Khangai Complex, to do detailed field investigation, and geochronological and geochemical analyses. This paper presents the results, which have important implications for the regional tectonic evolution.

GEOLOGICAL SETTINGS

The CAOB hosts a number of large batholiths formed during the Paleozoic and Mesozoic which are formed in the various geological environment, the most interesting products of this magmatism are granitoid batholiths of the Late Paleozoic-Early Mesozoic age because of their unique size and role during the late evolution of CAOB (Yarmolyuk et al., 2016).

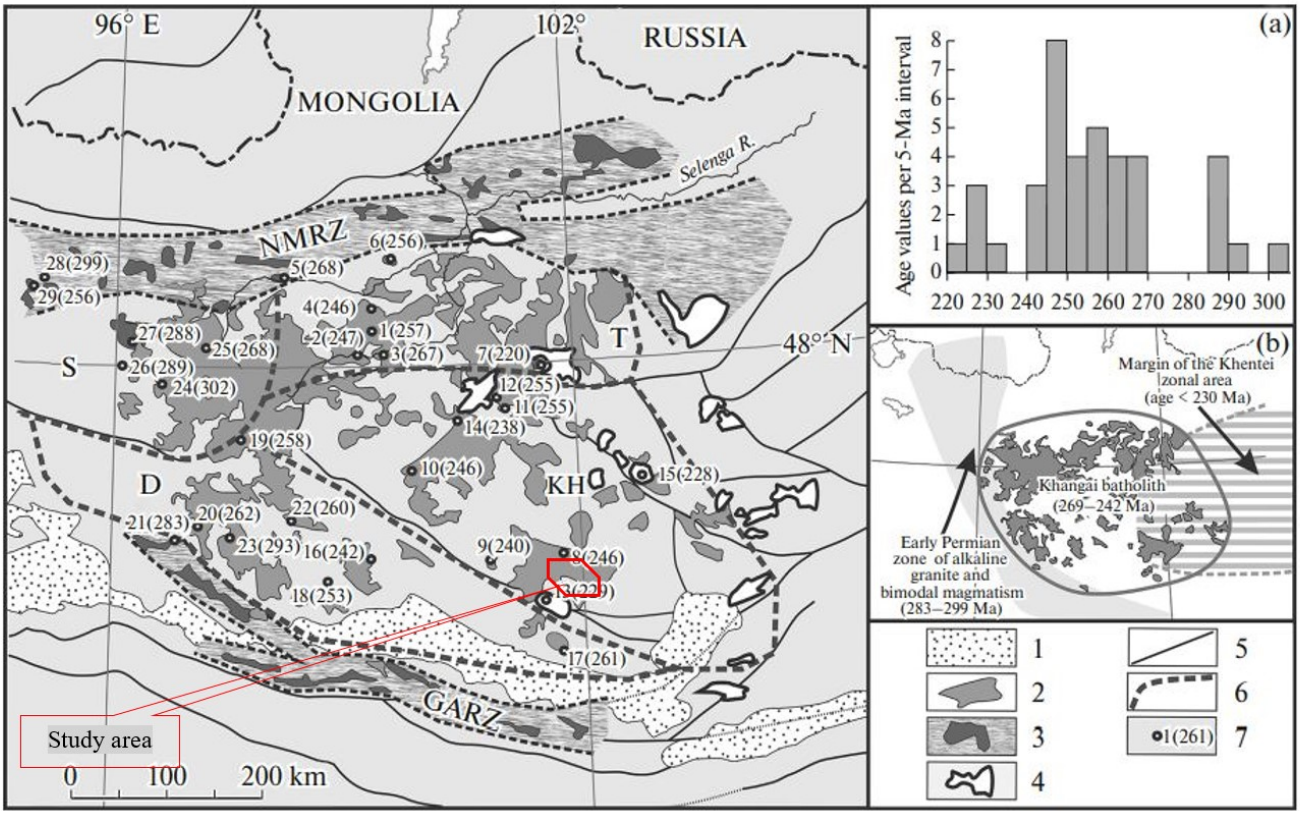

Fig. 1. Schematic geological map of the Khangai zonal magmatic area (Yarmolyuk et al., 2016). Legend: (1) Mesozoic and Cenozoic depressions; (2) granitoid massifs of the Khangai batholith; (3) rift zones (GARZ is the Gobi Altai rift zone and NMRZ is the northern Mongolian rift zone) and exposed bimodal volcanic associations and alkaline granites; (4) Late Triassic volcanic fields and granitoid massifs; (5) faults; (6) boundaries among the continental blocks or terranes (S-Songino, D-Zavkhan, T-Tarvagatai, KH-Khangai); (7) sampling sites for isotopic dating. (a) histogram showing the distribution of age values of granitoids in the Khangai batholith area; (b) schematic map showing the distribution of magmatic areas of various ages in the vicinity of the Khangai batholith.

The origin of the batholiths was closely related to alkaline and subalkaline complexes associated with Late Paleozoic-Early Mesozoic rift systems (Yarmolyuk and Kovalenko, 2003b).

The Permian-Early Triassic magmatic province generally comprises diverse magmatic complexes, which occur over an area of >4 million km^2 and one of its distinguishing features is zonal magmatic areas: Khangai, Barguzin, and Mongolia-Transbaikalia which consist of batholiths surrounded by coeval rift zones (Yarmolyuk et al., 2016; Yarmolyuk et al., 2013b).

The Khangai zonal magmatic area (Fig. 1) covers approximately 250000 km^2 and includes the Khangai batholith and the Gobi Altai and northern Mongolian rift zones that surround the batholith in the south and north (Yarmolyuk et al., 2016). The Khangai batholith occurs within a half of the magmatic area and is composed of a number of rock associations, which are dominated by granitoids of normal alkalinity grouped into the Khangai Complex and the

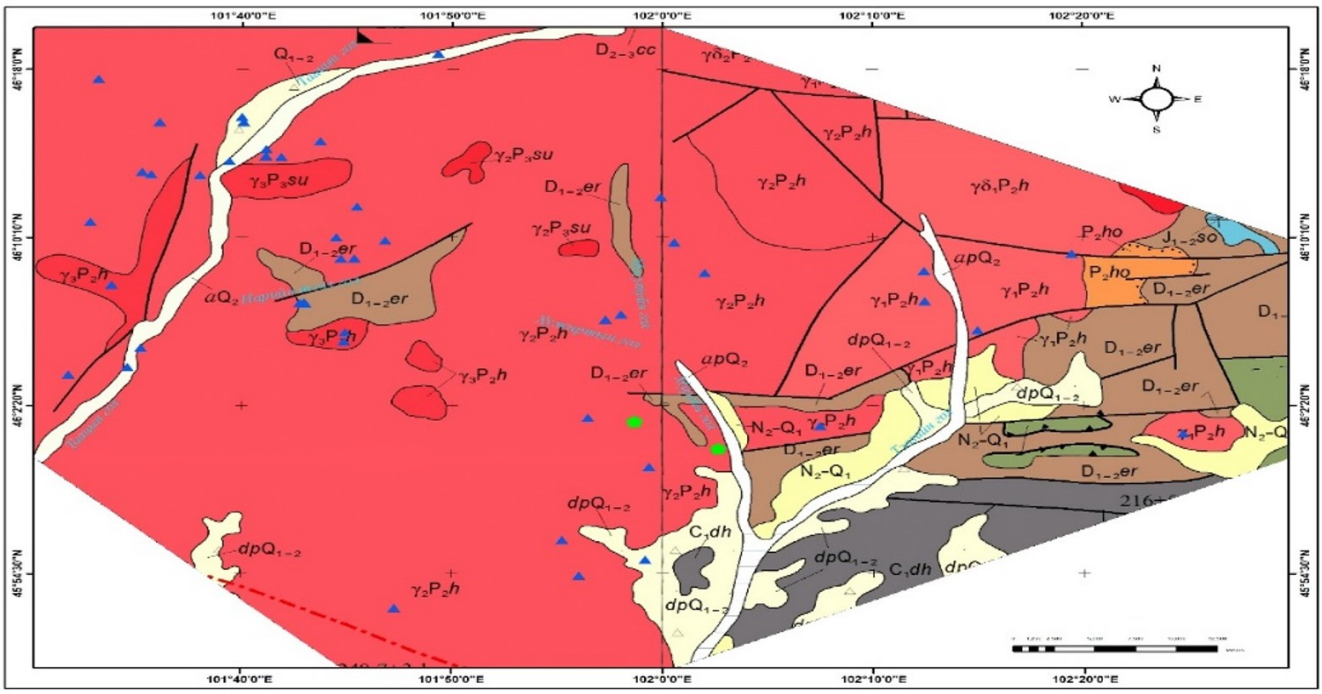

Legend

- apQ_2 Holocene: The lake originated pebbles, gravels, sandy and loam
- dpQ_{1-2} Upper pleistocene-holocene: Pebble, gravel and loam of side-trough, dry valleys and river valleys
- N_2-Q_1 Neogen-upper pleistocene: Reddish clay, sandly sediments
- $J_{1-2}so$ Lower-medium Jurassis. Saikhan-Ovoo Formation. Conglomerate, sandstone, tuff-sandstone
- γ_3P_3su Early permian.Shar-Usgol Complex. III phase. Leucogranite.
- γ_3P_2h Middle permian. Khangai Complex. III phase. Leucogranite, granite
- γ_2P_2h Middle permian. Khangai Complex. II phase. granodiorite
- C_1dh Mississippian. Dulaankhayrkhan Formation. terrigenous-sedimentary ,
- $D_{1-2}er$ Lower-medium devonian. Erdenetsogt Formation. Basalt, sandstone
- S-D_1cr Silurian-lower devonian. Tsoroidog Formation. Metachert, basalt
- Silicate and geochemical point
- Geochronological point

Fig. 2. Geological map of the study area

second most abundant rock type is subalkaline leucocratic granites of the Sharus Gol Complex (Fedorova, 1977; Dergunov et al., 2001). The granitoids are classified according to their composition into two magmatic associations: granite- granodiorite, which is made up mostly by rocks of the Khangai Complex, and granite-leucogranite, which corresponds to the Sharus Gol Complex (Yarmolyuk et al., 2016). Intrusive rocks of the Khangai Complex intrude the Carboniferous Tarvaragtai Complex in the western and northwestern parts and are intruded by Triassic leucogranites of the Sharus Gol Complex.

In the study area, the intrusive rocks of the Khangai Complex intruded the Silurian to Lower Devonian Tsoroidog Formation, the Lower-Middle Devonian volcanogenic-silicic-sedimentary rocks of the Erdenetsogt Formation, upper Devonian-Mississippian, the Mississippian terrigenous-sedimentary rocks of the Dulaankhairkhan Formation, and the Cisuralian volcanogenic rocks of the Khoshigt Formation. They are crosscut by the Triassic Sharus Gol Complex and late Jurassic to early Cretaceous subvolcanic dykes and covered by the early-mid Jurassic Saikhan-Ovoo Formation and Quaternary sediments. In the contact zones with the Erdenetsogt Formation, mafic volcanics are metamorphosed into amphibolite and amphibolic schist. The contact metamorphic zones are normally 5-10 m in width, usually with lesser content of dark minerals and finer-grained textures compared with the pluton (Fig. 2).

The Khangai Complex is comprised of several plutons, such as Taatsiin Gol (5000 km^2), Baits, Khanui, Mandal, Upper Orkhon (each 1000-2000 km^2) in Khangai area. The Taatsiin Gol pluton is the biggest (5000 km^2) and is representative of the Khangai Complex and is composed of three phases: the first phase of fine -medium grained, dark grey diorite, the second phase of coarse-grained, pinkish grey, porphyritic granodiorite and granite, and the third phase of fine-grained, light grey, biotite granite, and leucogranite (Orolmaa and Dolzodmaa, 2019).

METHODS

Field observation and study were conducted on the intrusive rocks of the Khangai Complex around the Uyanga area, with 10 samples selected for petrographic study, 32 samples for geochemistry, and 2 samples for zircon U-Pb dating.

Thin-section observations were conducted at the Geological Investigation Center, State owned Enterprise of Mongolia. Major and trace element analyses were performed by XRF and ICP-MS (for 56 elements), respectively, at the "SGS Mongolia" laboratory in accordance with the standardized methodology. Zircons used for U-Pb dating were contracted from fresh rock samples of ca. 2-3 kg by conventional heavy liquid method and the U-Pb isotope analysis was carried out by using the LA-ICPMS at the laboratory of the Institute of Mineral Resources, Chinese Academy of Geological Sciences. The internal structure of zircons was examined by using an optical microscopy at both the transmitting and reflective modes, and by cathode-luminescence (CL) imaging using a microprobe. The size of the target analytical spots is 32 μm in diameter and the concentrations of U, Th, and Pb were calibrated by using the 29Si internal standard.

RESULTS

Petrography

The first phase of the Taatsiin Gol pluton (Fig. 3) is made up of medium-grained diorite, the second phase includes fine-to medium-grained granodiorite, and the third phase is dominated by fine-medium grained biotite granite.

The first phase diorite of the Taatsiin Gol pluton is composed of plagioclase (63-66%), hornblende (20-25%), biotite (10%), a minor amount of K-feldspar (5%) and quartz (5-7%). The grain size of minerals reaches 1 mm x 2.5 mm. Plagioclase is prismatic and tabular, partly replaced by sericite and saussurite in the core of grains. Plagioclase composition is andesine (An_{30-35}) (Fig. 4).

The second phase of granodiorite (Fig. 5, 6) is porphyritic, with feldspar, plagioclase, hornblende, biotite phenocrysts in fine-grained matrix. The phenocrysts are common (around 50%) in the rock. The matrix is mainly

Fig. 3. Outcrop of the first phase diorite of Taatsiin Gol pluton Khangai Complex

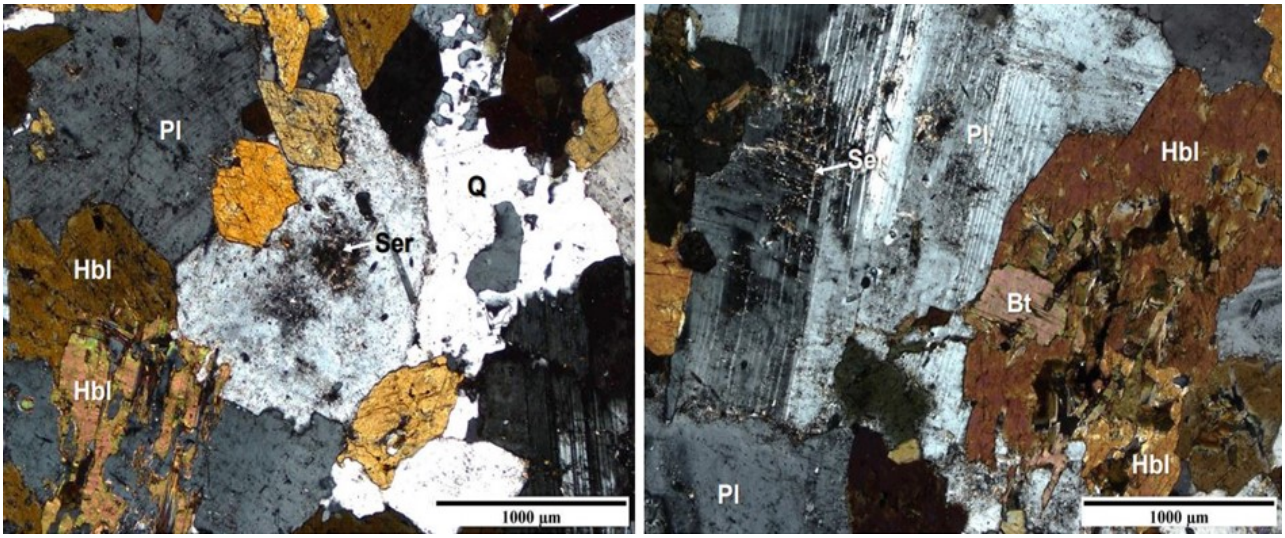

Fig. 4. Microphotograph of the first phase diorite, Taatsiin Gol pluton, Khangai Complex (Si-36)
Hbl- hornblende, Pl-plagioclase, Q-quartz, Bt-biotite, Ser-sericite.

composed of plagioclase (30-35%), hornblende (10-15%), quartz (15-20%), K-feldspar (10-15%), and biotite (10-15%) with accessory apatite, ore minerals and titanite. Plagioclase is the dominant mineral and occurs as tabular and prismatic crystals of 0.6-1.4 mm in size and have An_{30-32}. Plagioclase is partly replaced by sericite, leucoxenized ilmenite, and epidote aggregates. Large plagioclase grains poikilitically include amphibole and biotite (Fig. 7).

The third phase of the Taatsiin Gol pluton (Fig. 8) is porphyritic weak-gneissose granite consists of phenocrysts (20-30%) that are quartz, feldspar and matrix (70-80%). Also, the rock's matrix is mainly composed of K-feldspar (38-45%), quartz (30%), and plagioclase (20-25%), with a minor amount of biotite (5-7%). Accessory minerals are apatite, zircon, and titanite. Phenocrystals are represented by quartz, K-feldspar, and plagioclase. Quartz pegmatite intergrowth develops along the feldspar grain boundaries in the groundmass. Biotite flakes are elongated and define a foliated structure (Fig. 9). Meanwhile, small biotite flakes locally form clusters aligned to the foliation.

Fig. 5. Outcrop of second phase of Khangai Complex, Uyanga area

Fig. 6. Weathered second phase granite, Khangai Complex; Right photo: xenolith-bearing Bt-Hbl-granite

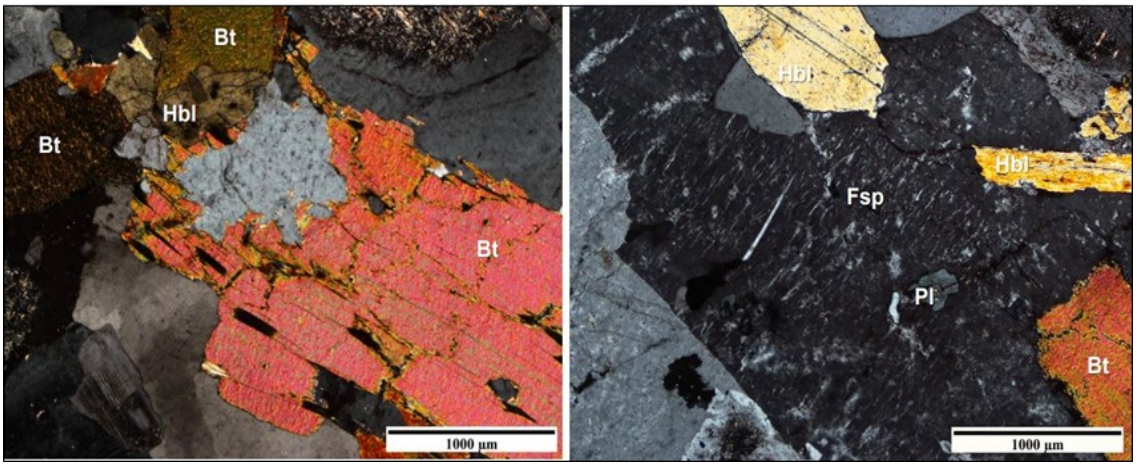

Fig. 7. Microphotograph of the second phase granodiorite, Taatsiin Gol pluton Khangai Complex (Si-41) Hbl-hornblend, Bt-biotite, Pl-plagioclase, Fsp- K-feldspar,

Fig. 8. Outcrop of the third phase of Khangai Complex

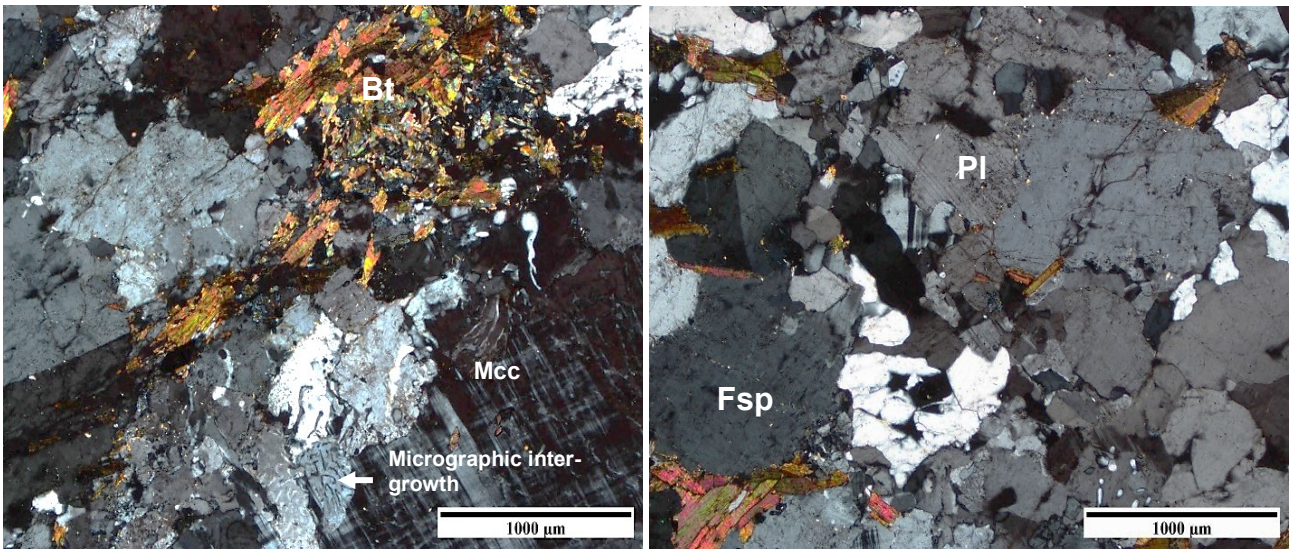

Fig. 9. Microphotograph of third phase biotite granite, Khangai Complex (Si-396), Bt-biotite, Pl-plagioclase

Geochemistry

In order to determine the geochemical characteristics of granitoid rocks of the Taatsiin Gol pluton a totally of 7 samples of first phase diorite, 20 samples of second phase granodiorite, and porphyritic biotite-hornblende granite and, 12 samples of third phase biotite granite were analyzed for major trace and rare earth elements. Representative samples of each phase are shown in Table 1.

The results show the major element contents are SiO_2 = 56.34-76.14 wt.%, Al_2O_3 = 11.39- 16.93 wt.%, MgO = 0.12-12.4 wt.%, CaO = 0.73-8.25 wt%, Na_2O = 1.47-5.34 wt.%, and Fe_2O_3 = 1.18-5.02 wt.%. In the total alkali-silica (TAS - Na_2O + K_2O vs SiO_2) diagram, the first phase samples plot in the subalkaline gabbro and diorite fields, the second phase rocks plot in the quartz-diorite and granite fields, and the third phase rocks plot into the granite and alkali granite fields (Fig.

Table 1. Chemical compositions of selected samples from the Taatsiin Gol pluton of Khangai Complex

Rock type	Quartz diorite	diorite		Granodi-orite	Bt-Hrb granite		Granite		
Phase		I			II			III	
Sample no.	Si-36	Si-3847	SH.H-5	Si-50	Si-6615	Si-6618	Si-46	Si-391	Si-13453
Major element (wt.%)									
SiO2	56.67	51.1	52.21	62.55	65.73	65.84	76.14	74.06	73.81
TiO2	1.593	1.59	0.92	0.64	0.46	0.44	0.09	0.275	0.21
Al2O3	16.28	13.82	11.39	15.22	16.17	16.09	12.89	13.92	13.83
Fe2O3	7.86	9.85	10.42	5.02	3.8	3.65	1.19	1.66	1.63
MnO	0.11	0.15	0.17	0.08	0.06	0.06	0.03	0.03	0.04
MgO	4.08	9.2	12.44	3.36	1.78	1.49	0.12	0.26	0.28
CaO	5.94	7.56	8.25	4.44	3.61	3.54	0.73	1.01	1.06
Na2O	3.41	2.82	1.47	3.75	4.04	4.01	3.7	3.10	3.58
K2O	2.46	2.17	1.29	2.97	2.78	3.1	4.67	4.96	5.22
P2O5	0.563	0.3	0.05	0.18	0.11	0.11	0.02	0.076	0.04
LOI	0.51	1.46	1.39	0.6	0.1	0.89	0.17	0.39	0.22
Total	99.5	100.02	100.00	98.81	98.64	99.21	99.75	99.73	99.91
Trace elements (ppm)									
Cs	8.3	6.6	2.5	5.7	1.4	2.9	8.2	5.1	12.1
Rb	81.5	72.5	47	101	73.5	83	332	270	309
Ba	802	609	404	636	698	812	121	400	564
Th	10.2	2.1	2.5	10.2	3	4.4	30.6	36.3	35.7
U	2.63	1.02	0.57	2.33	0.83	1.01	6.9	2.65	4.45
Ta	0.6	<0.5	<0.5	<0.5	<0.5	<0.5	2.3	0.7	1.6
Nb	14	7	3	6	5	5	14	8	14
La	46.8	29.4	11.7	28.4	18.6	24.5	23.1	75.1	51.5
Ce	95.3	62.1	26.3	53.5	35.6	47.7	49.6	102	138
Sr	910	672	235	500	399	414	57	180	133
Nd	44	33.5	26.3	21.2	14.6	16.6	19.6	44.7	35.2
Hf	5	4	2	4	4	4	3	5	4
Zr	213	147	81.2	163	155	132	81.8	191	138
Sm	9.2	7.6	3.8	4.2	3	3	5.2	7.6	6.8
Tb	0.74	0.85	0.53	0.41	0.31	0.3	0.81	0.46	0.68
Y	16.9	21.8	16.7	12.2	9.4	7.4	27.7	8.3	18.8
La	46.8	29.4	11.7	23.1	19	18	23.1	75.1	51.5
Pr	11.2	7.59	3.11	5.34	3.83	4.73	5.34	13.5	10.3
Nd	44	33.5	13.9	19.6	14.6	16.6	19.6	44.7	35.2
Eu	2.39	2	0.84	0.2	0.9	0.81	0.2	0.72	0.55
Gd	5.84	2.11	3.38	4.42	2.38	2.11	4.42	3.88	4.53
Dy	3.83	6.3	3.26	4.93	1.8	1.47	4.93	1.79	3.57
Ho	0.69	0.88	0.64	0.96	0.33	0.24	0.96	0.3	0.68
Er	1.69	2.21	1.81	2.83	0.98	0.69	2.83	0.78	1.8
Tm	0.22	0.28	0.26	0.42	0.12	0.1	0.42	0.09	0.25
Yb	1.6	1.9	1.9	2.6	0.9	0.7	2.6	0.5	1.7
Lu	0.19	0.26	0.27	0.43	0.13	0.1	0.43	0.06	0.25
Ga	21	19	13	20	19	18	20	22	20

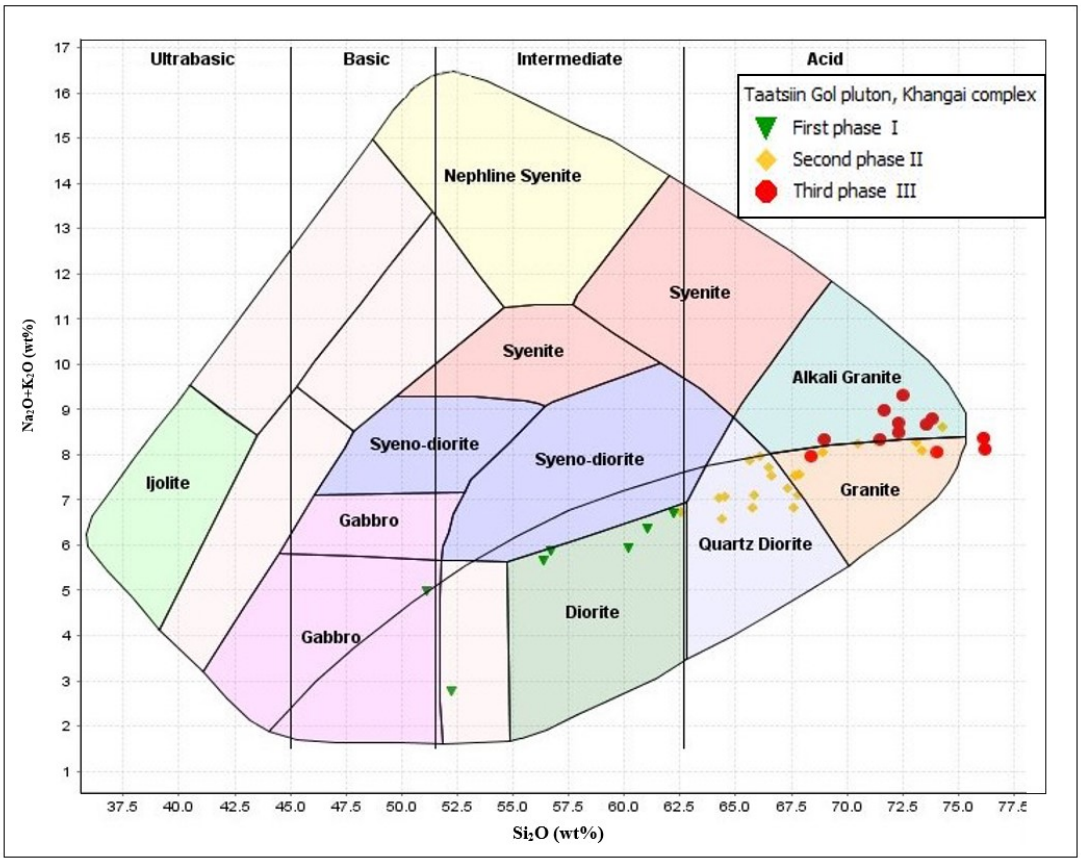

Fig 10. Total alkalis-silica (TAS) diagram for the Taatsiin Gol pluton Complex

10). Harker variation diagrams show a negative correlation of TiO_2, MgO, Fe_2O_3, CaO, MgO, and P_2O_5 against SiO_2, but a positive correlation of Na_2O and Al_2O_3 with SiO_2 (Fig. 11).

In the K_2O-Si_2O diagram (Rickwood, 1989), all the samples plot in the high-K calc-alkaline field (Fig. 12). According to the A/NKC vs C/NKC diagram, all the granitoids of the Taatsiin Gol pluton are metaluminous to weakly peraluminous, except for two samples of the third phase granite which plot in the strongly peraluminous field (Fig. 13). In the AFM diagram, the granitoids of the pluton show an obvious evolutionary trend of the calc-alkaline series (Fig. 14).

Primitive mantle-normalized trace element diagram shows that the granitoid rocks are depleted in high field strength elements (HFSEs) of Nb, Ta, Ti and Y and enriched in Cs, Rb, Th, and K (Fig. 15). The third phase granites of the Taatsiin Gol pluton, Khangai Complex display negative anomalies in Ba and Sr compared with the neighboring elements and are more richment in light rare earth elements (LREEs) and more intense negative Eu anomaly compared to the first and second phase rocks (Fig.16). In the diagram of the petrotectonic classification (Pearce et al., 1984), the Taatsiin Gol pluton samples of the first and the second phase rocks plot into the volcanic arc granite filed and the third phase granites into the syn-collision granite field (Fig.17). According to the FeO(T)-ASI classification diagram (Pearce et al., 1984) all the samples plot in the I-type granite field, except for 2 samples of the second and third phases falling in the S-type granite field (Fig. 18).

Geochronology

Two samples from third phase of the Taatsiin Gol pluton, one from granite (sample Si-391; GPS coordinates: N 45˚ 59'22.4" E 102˚ 04'3,4") and the other from biotite granite (sample Si-396; N 46˚00'40,6 E 102º02'44"). were selected for LA-ICPMS zircon U-Pb dating. Zircon grains from the biotite granite (sample Si-396)

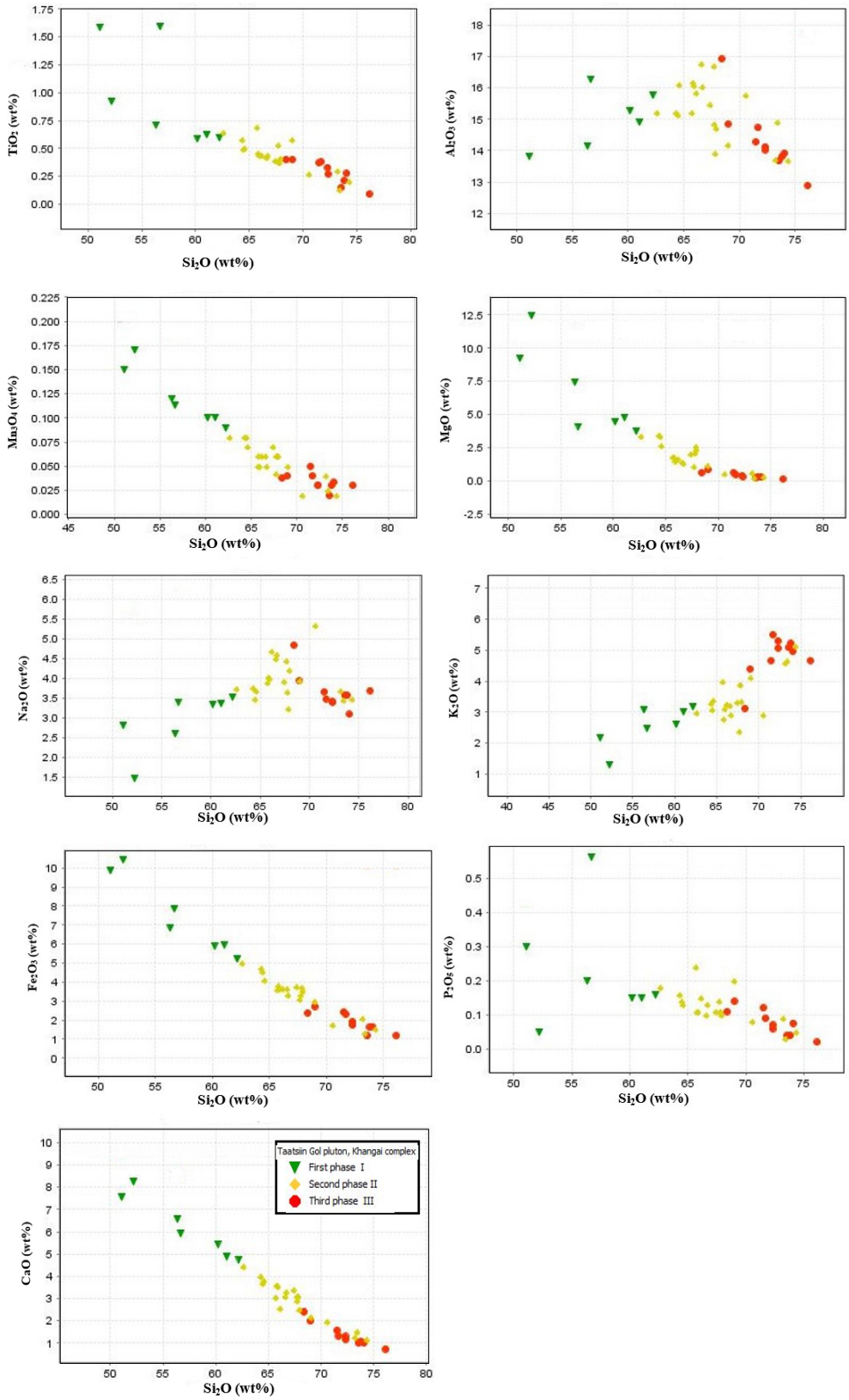

Fig. 11. Harker variation diagram for the Taatsiin Gol pluton

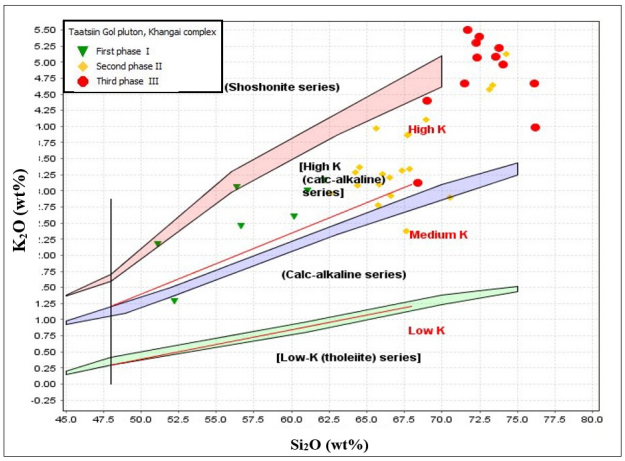

Fig 12. SiO2-K2O diagram (Rickwood, 1989)

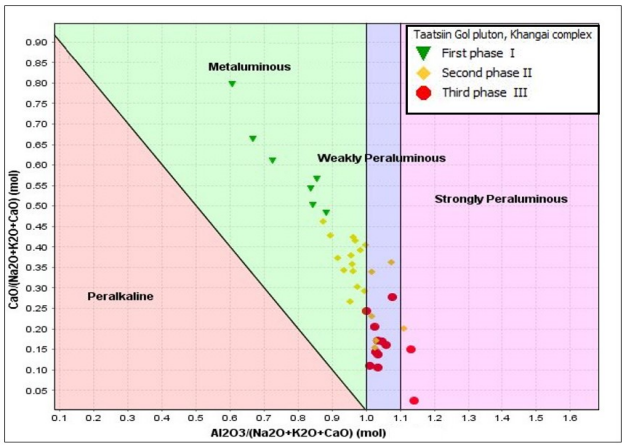

Fig 13. ASI diagram (Barton and Young, 2002)

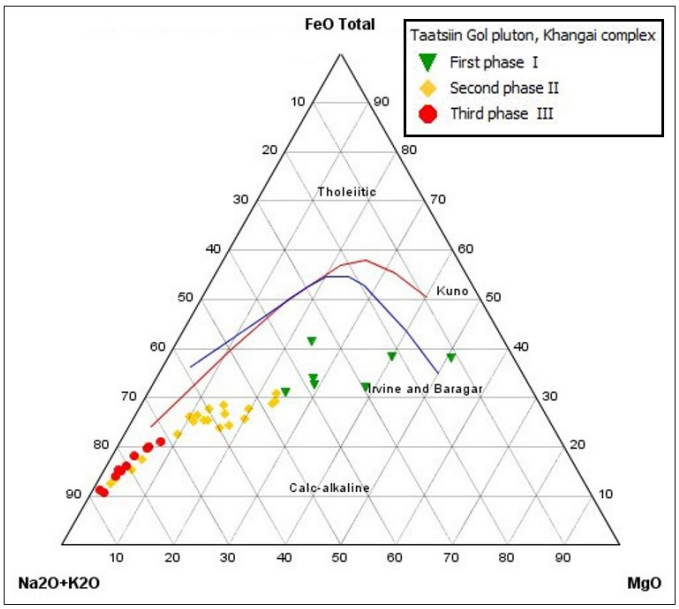

Fig 14. AFM diagram for the Taatsiin Gol pluton (Rollinson. 1993)

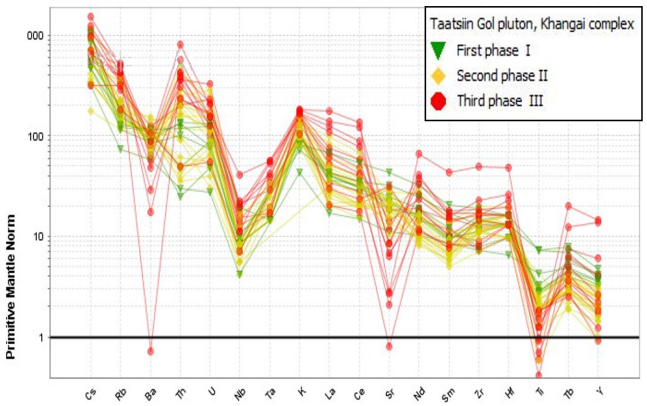

Fig 15. Primitive mantle normalized trace element spider diagram of Taatsiin Gol pluton, Khangai Complex (Sun and McDonough, 1989)

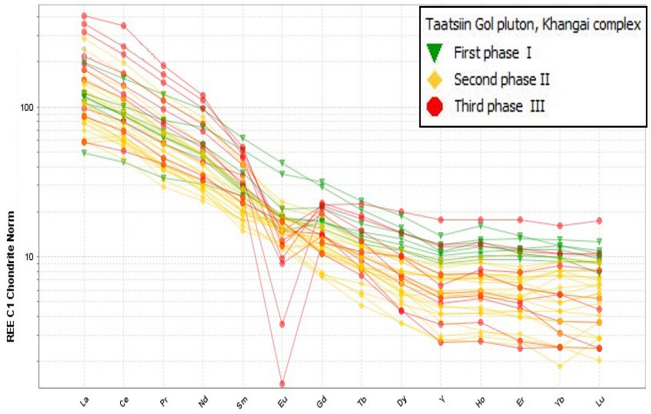

Fig 16. Chondrite normalized REE element spider diagram of Taatsiin Gol pluton, Khangai Complex (Sun and McDonough, 1989)

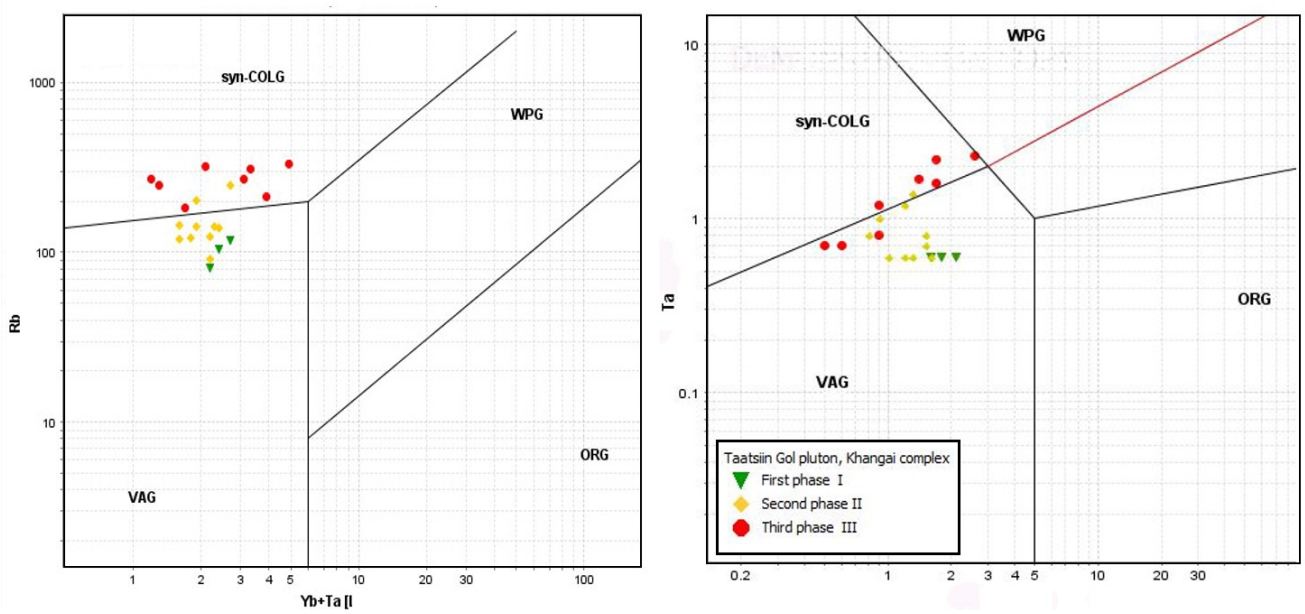

Fig 17. Tectonic discrimination diagram of the granite samples from Taatsiin Gol pluton, Khangai Complex (Pearce et al., 1984); syn-COLG-collision, WPG- within-plate, ORG-orogenic granite, VAG-volcanic arc granite

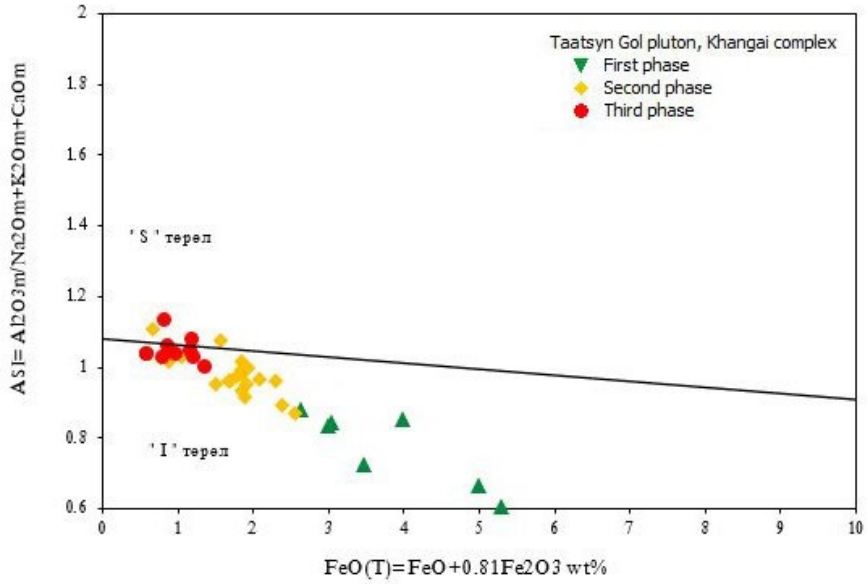

Fig 18. FeO (T) -ASI diagram of the Taatsiin Gol pluton, Khangai Complex (Pearce et al., 1984)

are elongate subhedral to prismatic and are 100-250 µm long. These zircons mostly show a core-overgrowth texture, with the cores displaying weak or no oscillatory zoning in CL images but the overgrowths having well-developed oscillatory zoning (Fig. 19A), which indicates an igneous origin for the zircon overgrowths, as well as the zircons. A total of 29 analyses were made on 20 zircon grains for this sample and all the analyses gave coherent results (Table 2), which yielded a weighted mean $^{206}Pb/^{238}U$ age of 241.4±1.2 Ma (MSWD = 0.99; Fig.19B).

Zircon grains from the biotite granite (sample Si -391), are essentially similar in internal texture, except for their relatively stubby morphology (Fig. 19C). Totally, 12 analyses were done on 12 zircon grains (Table 3). These analyses yielded a weighted mean $^{206}Pb/^{238}U$ age of 236.3±1.4 Ma (MSWD = 0.0016; Fig.19D).

Table 2. Isotope data of sample Si-391, Biotite granite from the Taatsiin Gol pluton, Khangai Complex

Samples	Th	U	$^{207}Pb/^{235}U$	$^{207}Pb/^{235}U$	$^{206}Pb/^{238}U$	$^{206}Pb/^{238}U$	$^{208}Pb/^{232}Th$	$^{208}Pb/^{232}Th$	$^{207}Pb/^{235}U$	$^{207}Pb/^{235}U$	$^{206}Pb/^{238}U$	$^{206}Pb/^{238}U$
	232	238	Ratio	1sigma	Ratio	1sigma	Ratio	1sigma	Age (Ma)	1sigma	Age (Ma)	1sigma
Si-391 biotite granite												
391-1	89.240	251.0624	0.243	0.0140	0.0375	0.000799	0.0105	0.000563	220.746	11.402	237.469	4.965
391-2	70.194	201.0202	0.238	0.0112	0.0375	0.000738	0.0105	0.000596	217.102	9.203	237.262	4.583
391-3	191.038	370.9175	0.261	0.0102	0.0371	0.000716	0.0108	0.000487	235.609	8.193	235.005	4.450
391-4	173.276	519.6204	0.264	0.0106	0.0378	0.000914	0.0114	0.000607	237.602	8.535	239.307	5.675
391-5	409.105	517.0428	0.250	0.0099	0.0367	0.000610	0.0106	0.000437	226.933	8.034	232.135	3.792
391-8	196.495	291.5810	0.280	0.0133	0.0383	0.000799	0.0113	0.000545	250.674	10.538	242.333	4.960
391-10	77.597	132.9610	0.297	0.0189	0.0375	0.000874	0.0117	0.000689	264.019	14.821	237.475	5.432
391-12	46.580	206.3084	0.250	0.0146	0.0373	0.000686	0.0115	0.000695	226.588	11.886	236.203	4.261
391-16	117.264	169.2156	0.279	0.0211	0.0374	0.000866	0.0121	0.000590	250.087	16.721	236.984	5.383
391-18	28.330	153.5412	0.292	0.0204	0.0374	0.000819	0.0117	0.001050	259.989	16.021	236.806	5.091
391-19	358.570	451.2290	0.277	0.0104	0.0376	0.000694	0.0121	0.000598	248.434	8.251	238.243	4.309
391-20	90.946	423.8423	0.273	0.0122	0.0375	0.000681	0.0111	0.000588	245.207	9.742	237.285	4.230

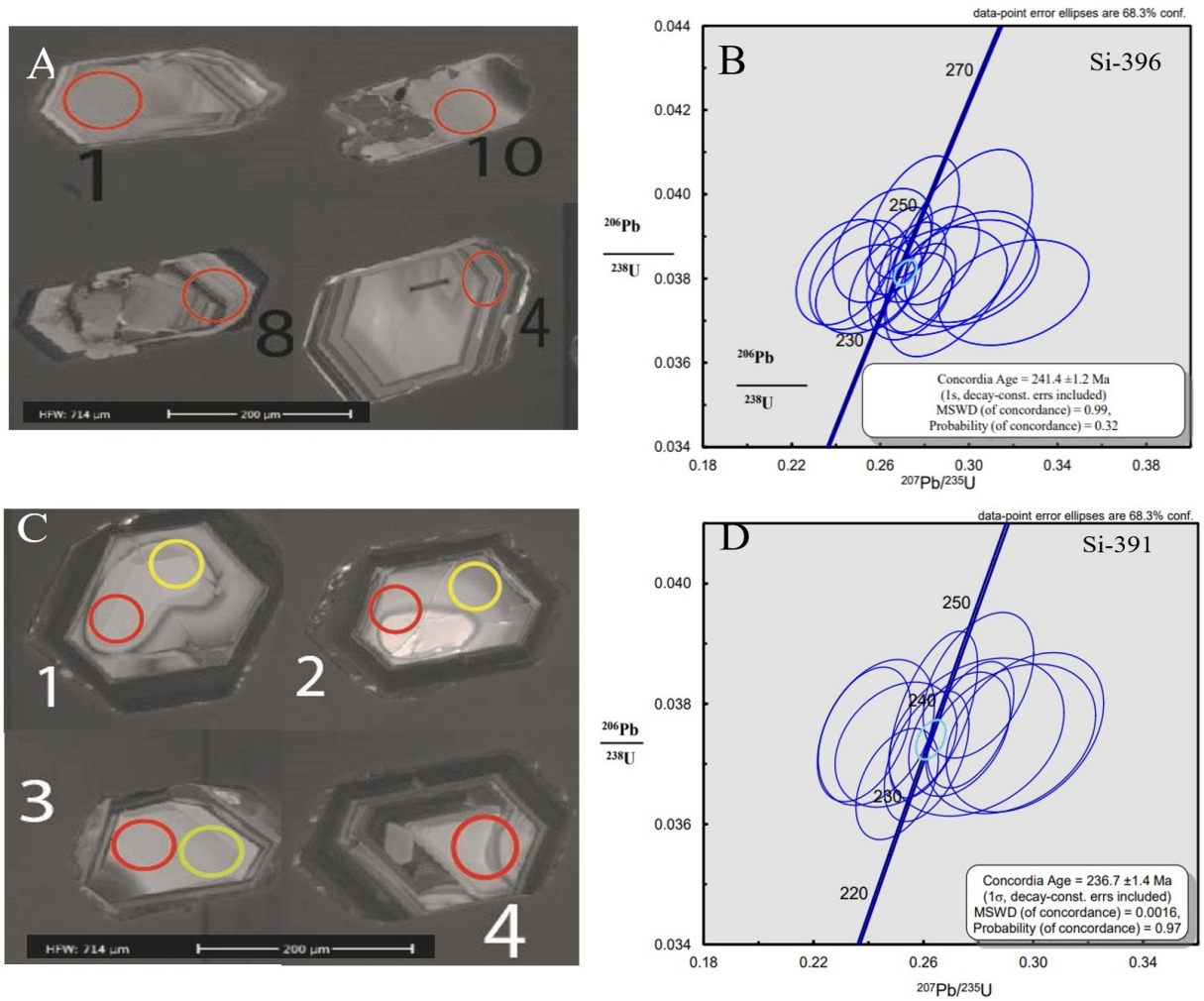

Fig 19. CL images as (a and c) and its concordia diagram (b and d) of the Taatsiin Gol pluton, Khangai Complex

Table 3. Isotope data of sample Si-396, Biotite granite from the Taatsiin Gol pluton, Khangai Complex

Samples	Th	U	$^{207}Pb/^{235}U$	$^{207}Pb/^{235}U$	$^{206}Pb/^{238}U$	$^{206}Pb/^{238}U$	$^{208}Pb/^{232}Th$	$^{208}Pb/^{232}Th$	$^{207}Pb/^{235}U$	$^{207}Pb/^{235}U$	$^{206}Pb/^{238}U$	$^{206}Pb/^{238}U$
	232	238	Ratio	1sigma	Ratio	1sigma	Ratio	1sigma	Age (Ma)	1sigma	Age (Ma)	1sigma
396-1	648.506	622.853	0.2684	0.00961	0.03866	0.000684	0.0124	0.000549	241.407	7.697	244.501	4.243
396-4	96.017	130.554	0.2504	0.01467	0.0381	0.000854	0.0118	0.000557	226.873	11.911	240.941	5.306
396-8	119.622	134.487	0.2856	0.02095	0.0379	0.000849	0.0112	0.000573	255.080	16.546	240.072	5.275
396-10	130.985	162.033	0.3202	0.02239	0.0377	0.000825	0.0102	0.000588	282.066	17.223	238.355	5.123
396-31	47.756	86.378	0.3005	0.01949	0.0383	0.000872	0.0135	0.000837	266.807	15.215	242.155	5.412
396-41	88.489	253.464	0.2435	0.01415	0.0382	0.000825	0.0104	0.000553	221.260	11.557	241.359	5.123
396-42	59.953	182.437	0.2611	0.01478	0.0388	0.000891	0.011	0.000671	235.552	11.899	245.295	5.529
396-43	200.439	384.989	0.2623	0.01083	0.0379	0.000732	0.011	0.000492	236.535	8.712	239.711	4.543
396-44	156.284	467.419	0.2754	0.01340	0.0395	0.000961	0.012	0.000618	247.018	10.667	249.452	5.958
396-45	450.309	542.226	0.2745	0.00993	0.0384	0.000627	0.0111	0.000453	246.257	7.909	242.843	3.891
396-48	209.499	298.683	0.2852	0.01284	0.0385	0.000769	0.0113	0.000541	254.781	10.142	243.803	4.776
396-52	46.580	206.308	0.2534	0.01485	0.0377	0.000698	0.0115	0.000698	229.321	12.032	238.856	4.334
396-57	291.345	655.728	0.2952	0.02205	0.0386	0.001622	0.012	0.000831	262.674	17.289	244.191	10.065
396-58	27.272	152.676	0.2990	0.02150	0.0381	0.000836	0.0119	0.001115	265.595	16.809	241.210	5.190
396-59	358.570	451.229	0.2783	0.01042	0.0378	0.000696	0.0121	0.000598	249.320	8.276	239.049	4.324
396-60	90.946	423.842	0.2739	0.01225	0.0376	0.000682	0.0111	0.000589	245.790	9.762	237.820	4.239
396-62	41.216	692.245	0.3032	0.01222	0.0380	0.000971	0.0162	0.001023	268.888	9.525	240.374	6.031
396-64	130.861	1366.983	0.2869	0.00804	0.0395	0.000905	0.0139	0.000626	256.146	6.342	249.984	5.613
396-65	136.580	1337.640	0.2756	0.00605	0.0390	0.000640	0.0127	0.000564	247.152	4.819	246.901	3.969
396-67	117.156	267.862	0.2709	0.01597	0.0388	0.000883	0.0129	0.000615	243.433	12.758	245.518	5.480
396-68	68.304	1352.754	0.2818	0.00644	0.0387	0.000691	0.0179	0.001085	252.090	5.099	245.063	4.291
396-69	47.364	681.425	0.2719	0.00833	0.0394	0.000770	0.0137	0.000863	244.209	6.648	249.051	4.775
396-70	37.225	693.815	0.2822	0.01158	0.0393	0.000832	0.0152	0.001213	252.364	9.169	248.632	5.162
396-71	43.026	961.135	0.2613	0.00797	0.0386	0.000958	0.0123	0.000852	235.717	6.414	244.207	5.948
396-73	12.456	258.017	0.2884	0.01329	0.0397	0.000831	0.0324	0.005141	257.332	10.472	250.902	5.154
396-75	128.070	258.140	0.2672	0.01183	0.0390	0.000706	0.0126	0.000563	240.463	9.478	246.536	4.383
396-76	41.177	693.793	0.2882	0.00836	0.0387	0.000615	0.0136	0.000814	257.161	6.591	244.987	3.817
396-78	129.294	1188.097	0.2825	0.00711	0.0393	0.000720	0.0123	0.000583	252.646	5.632	248.679	4.465
396-79	31.889	139.427	0.2550	0.01623	0.0387	0.000798	0.0114	0.000765	230.607	13.132	244.731	4.951

Table 4. Summary of age data of the Khangai Complex

Pluton name	Rock type	Sample	Age	Method	References
Taatsiin Gol	Biotite granite	Si391	236.3±1.4 Ma	U-Pb	This study
	Biotite granite	Si396	241.4±1.2 Ma	U-Pb	This study
	Porphyritic biotite-hornblend granite	XAH-09/46	246±2	U-Pb	Eenjin et al, 2017
	Biotite granite	15082002A	245.7±3.1	U-Pb	Dolzodmaa et al., 2020
	Granite		241	U-Pb	Yarmolyuk et al., 2013a,
	Granite	M-99-16	230	Rb-Sr	Jahn et al, 2004
	Granite	M-99-15	231	Rb-Sr	Jahn et al, 2004
Uyanga	Granite	52	242	U-Pb	Orolmaa and Erdenesaikhan, 2006
Erdenetsogt	Biotite granite	БХ-6/5	240±1	U-Pb	Eenjin et al., 2017
Gyatruun	Granite	O-49/02	245±4	U-Pb	Orolmaa and Erdenesaikhan, 2006
Egiin Davaa	Granite	XAH-06/1	246±10	U-Pb	Yarmolyuk et al., 2013a
Del Khad	Granodiorite	4702	255±5.1	U-Pb	Togtokh and Sukh-Erdene, 2009
Hyar	Granite	4701	252.1±7.2	U-Pb	Togtokh and Sukh-Erdene, 2009
Zaraa Tolgoi	Granodiorite	4700	247±7.8	U-Pb	
Yest Nuur	Porphyritic granite	6634	249.5±5.6	U-Pb	Uyakhan et al., 2017
Khukh Nuur	Porphyritic granite	6635	245.6±4.1	U-Pb	
Noyonkhangai	Granite	OR-15-07	253.8±1.3	U-Pb	
Chuluut	Granite	OR-21-07	255.56±0.95	U-Pb	
Burd	Granite	O-8/12	252.2±1.5	U-Pb	Orolmaa and Dolzodmaa, 2019
	Granite	O-12/04 (DH12)	241.3±1.5	U-Pb	

DISCUSSION

Formation time of the Khangai Complex

According to previous geochronological studies for granitoids in Central Mongolia and Bayankhongor districts, the Khangai and Sharus Gol complexes are considered to have different ages, with the Khangai Complex older than the Sharus Gol complex. However, both the complexes have been dated as 250 Ma (Takahashi et al., 2000). Some researchers explain that the Khangai Batholith is formed within the time span of 269-241 Ma (Yarmolyuk et al, 2016; Yarmolyuk et al, 2013a, 2013b). According to a later publication of granitoid plutons in the central and southern part of Khangai Complex intruded in 269-252 Ma (Mid-Late Permian) and 255-237 Ma (Early -Mid Triassic). They considered that it is appropriate to classify into two age complexes which are the Khangai Complex (269-252 Ma), and Egiin Davaa complex (255-237 Ma) (Orolmaa and Dolzodmaa, 2019). In our study, the third phase biotite granite of the Taatsiin Gol pluton (Khangai Complex) shows U-Pb zircon ages of 241.4±1.2 Ma and 236.7±1.4 Ma. Based on our new and published age data (Table 4), the age of the Taatsiin Gol pluton of the Khangai Complex in the Uyanga area is 256-230 Ma, consistent with late Permian to mid-Triassic time.

Tectonic settings

As aforementioned, granitoid rocks of the Taatsiin Gol pluton can be divided into three

phases according to the field relations and petrographical characteristics. The first phase is mainly characterized by fine-medium-grained diorite, the second phase is medium to coarse-grained, porphyritic biotite-hornblende granite and granodiorite, and the third phase is represented by biotite granite. In terms of geochemistry, all the rocks of the three phases belong to the high-K calc-alkaline series and I-type granites (Fig. 14 and Fig.18) although they display a gradual change in geochemical signature (Figs. 14-16).

The rocks of all the three phases contain relatively more contents of water-bearing minerals (e.g., hornblende and mica), implying formation in a subduction zone environment. If the high-K feature of these rocks is taken into consideration, we can further suggest that the subduction zone environment was likely confined to a continental arc or an active continental margin setting because the continental crust is enriched in K.

Geochemically, the rocks of the former two phases display major and trace element features similar to those of typical arc igneous rocks. For example, the rocks are depleted in HFSE such as Nb, Ta, Ti and Y and enriched in LILE such as Rb, Cs, Th, K and LREE. As a result, these features demonstrate that the first two phases of rocks were formed in an arc (or subduction zone) setting. The third phase rocks have similar trace element and REE patterns to the first two phase rocks, except for that they reveal more evident HFSE depletion and stronger negative anomalies of Ba, Sr, and Eu than the former two -phase rocks, suggesting that the latter rocks were generated from a source where plagioclase is a major residual phase, or the magmas experienced stronger plagioclase crystal fractionation. From the Harker diagrams (Fig. 13), it is certain that the third phase granites were not formed by crystal fractionation from the first two phase granites, as evidenced by the nonlinear relations of Na_2O and Al_2O_3 with SiO_2. Therefore, we believe that the highly negative Eu and Sr anomalies of the third phase granites resulted from the residence plagioclase in the source. In the case of plagioclase as a major residual phase, the magma source would be located at a relatively shallow crustal level. So, we propose that the third phase granites of the Taatsiin Gol pluton were also formed in a subduction setting.

Alternatively, granitoids forming in a post-collision environment can also show geochemical features similar to those of the third phase granites. Considering the very narrow age gap of the three phase intrusions of the Taatsiin Gol pluton (256-230 Ma), which seems to be too short for an orogenic belt to change from an oceanic plate subduction regime to a post-collision one, we prefer an active continental margin setting (subduction) for the third phase granites of the Taatsiin Gol pluton. In a word, the Taatsiin Gol pluton, as well as the whole Khangai complex, were most likely formed in an active continental margin setting.

Implications for the Mongol-Okhotsk Belt evolution

The Khangai area is located at the conjunction of two orogenic systems, the CAOB to the northeast and the Mongol-Okhotsk Belt to the south and west. Our new results and published data demonstrate that the intrusive rocks of the Khangai Complex were formed during the latest Permian and mid-Triassic period, and therefore the possibility that its formation was directly related to the subduction of the Paleo Asian Ocean plate can be precluded because the Khangai area belongs to the Early Paleozoic Domain of Mongolia the concurrent subduction zone of the during that time the Paleo Asian Ocean was located far south on the Mongolia-China border area (Sengor and Natal'in, 1996; Xiao et al., 2003).

Regarding the origin of the Khangai Complex, it has been intensely discussed in the literatures. Some researchers believe that it formed by convergence processes during the closure of the Mongol-Okhotsk Ocean (e.g., Donskaya et al., 2012; Yarmolyuk et al., 2016); some others explain that it was formed due to mantle plume (Yarmolyuk et al., 2016; Yarmolyuk et al., 2013b; Yarmolyuk and Kovalenko, 2003a, 2003b; Kuzmin et al., 2010), while there is a suggestion about a gradual change in the geodynamic environment from collision to intraplate setting (Litvinovsky et al., 2011). Recently, Dolzodmaa et al. (2020) concluded

that ~237 Ma granitoid magmatism in the Khangai area is related to the post-collisional environment in Mongol-Okhotsk Belt whereas Ganbat et al. (2021) proposed that late early Mesozoic granitoids (~230 Ma) in the Khangai-Khentii basin, Central Mongolia, were probably formed during the southward subduction of the Mongol-Okhotsk Ocean lithosphere.

As mentioned above, the third phase rocks of the Taasiin Gol pluton show geochemical features of post- or syn-collisional granites, and this geochemical characteristic is mainly caused by its shallow source region and thus does not change the explanation of the subduction geodynamic setting for the Taatsiin Gol pluton. As a consequence, we urge that the whole Khangai Complex were likely formed in a subduction zone environment during the latest Permian to the mid-Triassic period (256-230 Ma).

SUMMARY

The Taatsiin Gol pluton of the Khangai Complex contains intrusive rocks of three phases. The first phase is composed mainly of diorite, the second phase consists of fine-to medium-grained granodiorite and granite, and the third phase comprises fine to medium-grained biotite granite. Although showing variated geochemical features, the rocks of the three phases are all suggested to form at an active continental margin setting, probably related to the southwestward subduction of the Mongol-Okhotsk Ocean plate during the late Permian to mid-Triassic period.

ACKNOWLEDGEMENT

Acknowledgement Authors thank to reviewers for their valuable improvement of our manuscript. We also thank to researcher A.Chimedtseren for his suggestion in discussion. The first author is grateful to the staffs of the Gurvan Undes Company Ltd for their constant support and assistance. She also thanks to the company for the financial support for her Master study.

REFERENCES

Badarch, G., Cunningham, W.D., Windley, B.F. 2002. A new terrane subdivision for Mongolia: Implications for the Phanerozoic crustal growth of Central Asia. Journal of Asian Earth Sciences, v. 21, p. 87-104. https://doi.org/10.1016/S1367-9120(02)00017-2

Barton, M.D., Young, S., 2002. Non-pegmatitic deposits of beryllium: mineralogy, geology, phase equilibria and origin in E.S. Grew, ed., Beryllium: Mineralogy, Petrology and Geochemistry: Reviews in Mineralogy and Geochemistry, v. 50, p. 591-691. https://doi.org/10.2138/rmg.2002.50.14

Dergunov, A.B., Kovalenko, V.V., Ruzhentsev, S.V., Yarmolyuk, V.V. 2001. Tectonics, Magmatism, and Metallogeny of Mongolia, London-New York: Routledge, Taylor and Francis Group, 2001.

Dolzodmaa, B., Osanai, Y., Nakana, N., Adachi, T. 2020. Zircon U-Pb geochronology and geochemistry of granitic rock in central Mongolia. Mongolian Geoscientist, v. 50, p. 23-44. https://doi.org/10.5564/mgs.v50i0.1327

Donskaya, T.V., Gladkochub, D.P., Mazukabzov, A.M., De Waele, B., Presnyakov, S.L. 2012. The Late Triassic Kataev volcano-plutonic association in western Transbaikalia, a fragment of the active continental margin of the Mongol-Okhotsk Ocean. Russian Geology and Geophysics, v. 53(1), p. 22-36. https://doi.org/10.1016/j.rgg.2011.12.002

Eenjin, G., and Yarmolyuk, V.V. 2017. Problems of age and origin of granitoids in Central Mongolia. Khaiguulchin 57, p.62-67 (in Mongolian).

Fedorova, M.E. 1977. Geologicheskoe polozhenie i petrologiya granitoidov Khangaiskogo batolita (Geological Setting and Petrology of Granitoids of the Khangai Batholith), Moscow: Nauka (in Russian).

Ganbat, A., Tsujimori, T., Miao, L., Safonova, I., Pastor-Galan, D., Anaad, Ch., Baatar, M., Aoki, Sh., Aoki, K., Savinskiy, I. 2021. Late Paleozoic-Early Mesozoic granitoids in the Khangay-Khentey basin, Central Mongolia: Implication for the tectonic evolution of the Mongol-Okhotsk Ocean margin. https://doi.org/10.31223/X57S5D

Jahn, B.M., Capdevila, R., Liu, D.Y., Badarch, G., 2004. Sources of Phanerozoic granitoids in Mongolia: geochemical and Nd isotopic

evidence, and implications for Phanerozoic crustal growth. Journal of Asian Earth Sciences, v. 23, p. 629-653. https://doi.org/10.1016/S1367-9120(03)00125-1

Kuzmin, M.I., Yarmolyuk, V.V., Kravchinsky, V.A. 2010. Phanerozoic hot spot traces and paleogeographic reconstructions of the Siberian continent based on interaction with the African large low shear velocity province, Earth Science Review, v. 102, p. 29-59. https://doi.org/10.1016/j.earscirev.2010.06.004

Litvinovsky, B.A., Tsygankov, A.A., Jahn, B.M., Katzir, Y., Be'eri-Shlevin, Y. 2011. Origin and evolution of overlapping calc-alkaline magmas: the late Palaeozoic post-collisional igneous province of Transbaikalia (Russia). Lithos 125, p. 845-874. https://doi.org/10.1016/j.lithos.2011.04.007

Orolmaa, D., Dolzodmaa. B, 2019. Zircon U-Pb geochronology and geochemistry of granitic rock in Khangain. Khaiguulchin, 61, p. 119-130 (in Mongolian).

Orolmaa, D., Erdenesaihan, G., Borisenko, A.S., Fedoseev, G.S., Babich, V.V., Zhmodik, S.M. 2008. Permian-Triassic granitoid magmatism and metallogeny of the Khangain (central Mongolia). Russian Geology and Geophysics, v. 49(7), p. 534-544. https://doi.org/10.1016/j.rgg.2008.06.008

Orolmaa, D., Erdenesaikhan, G. 2006. To problems of Khangai granitoids. Proceedings of Institute of Geology and Mineral Resources, v. 16, p. 47-70 (in Mongolian).

Pearce, J.A., Harris, N.B.W., Tindle, A.G. 1984. Trace element discrimination diagrams for the tectonic interpretation of granitic rocks. Journal of Petrology, v. 25(4), p. 956-983. https://doi.org/10.1093/petrology/25.4.956

Rickwood, P.C 1989. Boundary lines within petrologic diagrams which use oxides of major and minor elements: Lithos, v. 22(4), p. 247-263. https://doi.org/10.1016/0024-4937(89)90028-5

Rollinson, H.R. 1993. Using Geochemical Data: Evolution, Presentation, Interpretation. Routledge, 384 p.

Sengor, A.M.C., Natal'in, B.A., 1996, Palaeotectonics of Asia: fragments of a synthesis, in Yin, A., Harrison, M., eds., Tectonic evolution of Asia: Cambridge, Cambridge University Press, p. 486-640.

Sun, S.S., McDonough. W.F, 1989. Chemical and isotopic systematics of oceanic basalt: implications for mantle composition and processes in Saunders, A.D., Norry. M.J., (Eds.), Magmatism in Ocean Basin Geological Society of Special Publication, London, p. 313-345. https://doi.org/10.1144/GSL.SP.1989.042.01.19

Takahashi, Y., Arakawa, Y., Oyungerel, S., Naito, K. 2000. Geochronological data of granitoid in the Bayankhongor area, central Mongolia. Bulletin of the Geological Survey of Japan, v. 51 (5), p. 167-174.

Togtokh, D., Gurtsoo, S., Lkhundev, Sh. 1984. Report on geological mapping at the scale 1:200 000 by Gurvansaikhan geological party in L-48-VII, XIV, L-48-XIII, XIX, XX, XXV, XXVI, XXXI, XXXII, K-48-I, II lists. #3912 (in Mongolian).

Togtokh, J., Sukh-Erdene, D. 2009. Geological mapping and general prospecting at the scale 1:50000 in Mogoit Khairkhan area in 2006-2009. #6070

Tumurchudur, Ch., Ganbat, D., Noosoi, Z. 1990. Report on geological mapping at the scale 1:200 000 by Galuut 2nd geological party. #4415.

Uyakhan, Z., Batbayar, Kh., Puntsagdulam, Ts., Banzragch, N., Enkhbold, N., Budsuren, B., Telmenbayar, A., Gantulga, B. 2016. Report on 1:50000 geological mapping and general prospecting work done in 2013-2016 in the Khukhnuur-50 project area covering Chuluut and Khangai soums of Arkhangai, Gurvanbulag and Jargalant soums of Bayankhongor aimag. Report #8150.

Windley, B.F., Alexeiev, D., Xiao, W., Kröner, A., Badarch, G. 2007. Tectonic models for accretion of the Central Asian Orogenic Belt. Journal of the Geological Society, v. 164, p. 31-47. https://doi.org/10.1144/0016-76492006-022

Xiao, W. Sun, M. Santosh, M. 2015. "Continental reconstruction and metallogeny of the Circum-Junggar areas and termination of the southern Central Asian Orogenic Belt". Geoscience Frontiers. v. 6(2), p. 137-140. https://doi.org/10.1016/j.gsf.2014.11.003

Xiao, W.J., Windley, B.F., Hao, J., Zhai, M.G. 2003. Accretion leading to collision and the

Permian Solonker suture, Inner Mongolia, China: Termination of the Central Asian Orogenic Belt, Tectonics, 22(6), 1069. https://doi.org/10.1029/2002TC001484

Yarmolyuk, V.V., Kovalenko, V.I. 2003a. Batholiths and geodynamics of batholith formation in the Central Asian fold belt, Russian Geology and Geophysics, v. 44(12), p. 1260-1274.

Yarmolyuk, V.V., Kovalenko, V.I. 2003b. Deep geodynamics and mantle plumes: their role in the formation of the Central Asian Fold Belt, Petrology, v. 11(6), p. 504- 531.

Yarmolyuk, V.V., Kovalenko, V.I., Kozakov, I.K., Sal'nikova, E.B., Bibikova, E.V., Kovach, V.P., Kozlovsky, A.M,. Kotov, A.B., Lebedev, V.I., Eenjin, G., Fugzan, M.M. 2008. The age of the Khangai batholith and the problem of batholith formation in Central Asia. Doklady Earth Sciences, v. 423, p. 1223 -1228. https://doi.org/10.1134/S1028334X08080096

Yarmolyuk, V.V., Kozlovsky, A.M., 2013. Age of the Khangai Batholith and the Problems of Polychronous Batholith Formation in Central Asia. V .452(6), p. 646-652. https://doi.org/10.1134/S1028334X13100176

Yarmolyuk, V.V., Kozlovsky, A.M., Sal'nikova, E.B., Kozakov, I.K., Kotov, A.B., Lebedev, V.I., Eenjin, G. 2013a. Age of the Khangai Batholith and Challenge of Polychronic Batholith Formation in Central Asia, Doklady Earth Sciences, v. 452, p. 1001-1007. https://doi.org/10.1134/S1028334X13100176

Yarmolyuk, V.V., Kozlovsky, A.M., Savantenkov. V.M., Kovach, V.P., Kozakov, I.K., Kotov. A.B., Lebedev, V.I., Eenjin, G. 2016. Composition, sources and geodynamic nature of giant batholiths of Central Asia, according to geochemical and Nd isotopic studies of granitoids of the Khangai zonal magmatic area. Petrology, v. 24, p. 433-461. https://doi.org/10.1134/S0869591116050064

Yarmolyuk, V.V., Kuzmin, M.I., Kozlovsky, A.M. 2013b. Late Paleozoic-Early Mesozoic within-plate magmatism in north Asia: traps, rifts, giant batholiths, and the geodynamics of their origin, Petrology, v. 21(2), p. 101-126. https://doi.org/10.1134/S0869591113010062

Zabotkin, L.V., Mosiondz, K.A., Dobrov, G.M. 1988. Report on geological mapping at the scale 1:200 000 in Bayankhongor area (L-47-XII,XXIII,XXIV, XXVIII, XXIX, XXX,XXXIV, XXXV, XXXIV lists). #4276 (in Russian).